Heme *b* quotas are low in Southern Ocean phytoplankton

Martha Gledhill*[1,2,3], Loes J. A. Gerringa[2], Patrick Laan[2] and Klaas R. Timmermans[2]

[1] Ocean and Earth Science, University of Southampton, National Oceanography Centre, Southampton, SO14 3ZH, UK

[2] Department of Biological Oceanography, Royal Netherlands Institute for Sea Research, PO Box 59, AB Den Burg (Texel), The Netherlands

[3] GEOMAR Helmholtz Centre for Ocean Research Kiel, Wischhofstr. 1-3, 24148 Kiel, Germany

*Corresponding author: mgledhill@geomar.de

Running head: Heme in Southern Ocean phytoplankton

1. Abstract

Heme is the iron containing prosthetic group of hemoproteins, and is thus required for photosynthesis, respiration and nitrate reduction in marine phytoplankton. Here we report concentrations of heme *b* in Southern Ocean phytoplankton and contrast our findings with those in coastal species. The concentration of particulate heme *b* (pmol L^{-1}) observed at the end of the exponential growth phase was related to the concentration of dissolved iron in the culture media. Small Southern Ocean phytoplankton species (< 6 µm in diameter) had heme *b* quotas < 1 µmol mol^{-1} carbon, the lowest yet reported for marine phytoplankton. Heme *b* was also depleted in these species with respect to chlorophyll *a*. We calculated the amount of carbon accumulated per mole of heme *b* per second in our cultures (heme growth efficiency, HGE) and found that small Southern Ocean species can maintain growth rates, even while heme *b* content is reduced. Small Southern Ocean phytoplankton can thus produce more particulate carbon than larger Southern Ocean or small coastal species at equivalent iron concentrations. Combining primary productivity and heme *b* concentrations reported for the open ocean, we found that HGE in natural populations was within the range of our laboratory culture results. HGE was also observed to be higher at open ocean stations characterized by low iron concentrations. Our results suggest that low heme *b* quotas do not necessarily result in reduced growth and that marine phytoplankton can optimize iron use by manipulating the intracellular hemoprotein pool.

2. Introduction

Iron is an essential nutrient for life but is present at very low concentrations, typically less than 200 pmol L^{-1}, in open ocean surface waters (De Baar & De Jong 2001). As a result of low ambient iron concentrations open ocean phytoplankton may have lower intracellular iron quotas than coastal species (Sunda et al. 1991, Sunda & Huntsman 1995, Strzepek et al. 2011), optimize their iron use via reduction of iron rich proteins (Strzepek & Harrison 2004), or exchange of iron containing proteins with non-iron containing alternatives (Erdner et al. 1999, Peers & Price 2006). Such changes appear to result in increased efficiency of growth in low iron environments (Raven 1988, 1990, Strzepek et al. 2011).

The major iron containing protein pools in phytoplankton are dominated by proteins involved in photosynthesis, nitrate reduction and respiration (Raven 1988, Strzepek & Harrison 2004). Hemoproteins are involved in electron transport and catalysis, and in the control, storage and transport of oxygen and other small molecules (Hogle et al. 2014). Hemes, the prosthetic groups of hemoproteins, contain one iron ion per molecule and many hemoproteins contain multiple hemes (Smith et al. 2010). Hemes are synthesized on the same biosynthetic pathway as chlorophyll and the molecules are related via their common tetrapyrrole ring structure (Tanaka & Tanaka 2007). Free heme is toxic (Espinas et al. 2012), so cellular heme concentrations are tightly regulated via complex feedback mechanisms that control tetrapyrrole synthesis (Tanaka & Tanaka 2007), and via heme oxygenase enzymes, which break down heme into biliverdins and iron (Shekhawat & Verma 2010). The heme iron reservoir could represent as much as 40 % of the total intracellular iron pool in marine phytoplankton (Raven 1988, Honey et al. 2013), in circumstances where iron storage is not significant.

Heme can also be a direct source of iron for marine bacteria, and there is evidence to suggest that marine bacteria utilize specific uptake pathways in order to directly access this source of iron (Hopkinson et al. 2008, Roe et al. 2013, Hogle et al. 2014). Hemoprotein concentrations are known to vary in response to iron availability, and intracellular iron concentrations have been shown to be a controlling factor for the biosynthesis of tetrapyrroles (Qi & O'Brian 2002). Diurnal cycling of hemoproteins in diazotrophic cyanobacteria (Saito et al. 2011), and increases in heme oxygenase in red algae (Richaud & Zabulon 1997) have been observed, suggesting that the heme-iron pool may represent a relatively mobile intracellular iron reservoir. Intracellular heme concentrations of marine phytoplankton growing in low iron environments might therefore be expected to be reduced, with potential impacts both on iron demand and heme requiring metabolic processes such as photosynthesis or nitrate reduction (Hogle et al. 2014).

Heme *b* (iron protoporphyrin IX) is perhaps the most versatile and ubiquitous heme, and is incorporated into hemoproteins such as the globins, cytochromes, catalase and oxidases. In phytoplankton, heme *b* makes up between 1 and 40% of the total cellular iron pool (Honey et al. 2013). However, no studies on heme abundance or regulation have so far been reported for species isolated from iron limited regions of the ocean, although Gledhill et al. (2013) have shown that concentrations of heme *b* in particulate material in the iron limited high latitude North Atlantic and in the Southern Ocean are deplete compared to more iron replete regions like the tropical North Atlantic. There is thus a need to examine the heme *b* quotas in phytoplankton species originating from low iron regions of the ocean in order to better understand how marine phytoplankton modify their heme *b* protein pool when growing at low iron concentrations.

The aim of our study was therefore to investigate heme *b* abundance in eukaryotic phytoplankton species isolated from the Southern Ocean, one of the lowest iron environments in

the ocean. We determined the concentrations of heme *b* accumulated in phytoplankton grown in Southern Ocean seawater at the end of the exponential growth phase. We compare heme *b* to iron concentrations in the cultures, to particulate organic carbon (POC) and to chlorophyll *a* (chl *a*). We utilized the concept of heme growth efficiency (HGE), which, in analogy to Raven (1988) and Strzepek et al. (2011), we defined as the moles of C fixed per mole of heme *b* per second. In this way we examined the overall impact of reduced heme content on carbon fixation in our phytoplankton cultures. We compared HGE calculated for our Southern Ocean phytoplankton with that calculated from heme *b* concentrations and primary productivity data for three sets of previously published field data from contrasting regions – the Celtic Sea (Hickman et al. 2012, Honey et al. 2013), the Scotia Sea (Korb et al. 2012, Gledhill et al. 2013) and the Iceland Basin (Poulton et al. 2010, Gledhill et al. 2013) to assess the relationship between low heme *b* and phytoplankton productivity in the ocean.

3. Materials and Methods

3.1 Phytoplankton growth conditions

Batch cultures of *Phaeocystis antarctica* (CCMP 1871, isolated from the Bellinghausen Sea), *Chaetoceros brevis* (CCMP 163, isolated from the Southern Ocean), *C. dichaeta* (NIOZ culture collection, isolated from the Southern Ocean) and *P. globosa* (NIOZ culture collection, isolated from the North Sea) were grown in triplicate in filtered Southern Ocean seawater (SOs, 0.2 µm, Sartobran, Sartorius) previously collected using trace metal clean sampling techniques from south of the Polar Front from a depth of 2-3 m using a "fish" towed from RV Polastern (Expedition 18/2, November 2000). Cultures were maintained in acid washed (1 mol L^{-1} hydrochloric acid) and Milli-Q water rinsed, microwave sterilized polycarbonate bottles

(Kawachi & Noel 2005). Sample and culture manipulations were carried out in a class 100 laminar flow hood following trace metal clean protocols (Sunda et al. 2005). Southern Ocean seawater was amended with the siderophore desferrioxamine (DFB, 5 nmol L^{-1}, Sigma) or $FeCl_3$ (5 nmol L^{-1}) to create three treatments SOs, SOs+DFB and SOs+Fe. *Phaeocystis globosa* and *C. calcitrans* (CCMP 1315, isolated from Japanese coastal waters) were grown in enriched SOs, which contained added ethylenediaminetetraacetic acid (EDTA, 100 µmol L^{-1}), cobalt (50 nmol L^{-1}), molybdenum (100 nmol L^{-1}), copper (20 nmol L^{-1}), manganese (115 nmol L^{-1}), zinc (80 nmol L^{-1}), selenium (10 nmol L^{-1}) and f/2 vitamins. Iron was added separately from a stock solution of 45 µmol L^{-1} FeEDTA to obtain final concentrations of 9, 15, 45 and 150 nmol L^{-1}. All experiments were carried out using a 16:8 h light:dark cycle under cool white fluorescent lights at 60 µmol quanta m^{-2} s^{-1}. *Phaeocystis antarctica*, *C. brevis* and *C. dichaeta* were grown at 4 °C, *P. globosa* at 15 °C and *C. calcitrans* at 22 °C. Cultures were maintained in experimental media for > 6 generations prior to experiments. For consistency, and to avoid issues arising from colony formation in both *Phaeocystis* species, growth rates for all species were calculated from the slope of the natural log (F_0, autofluorescence) obtained for dim-light adapted (15 min) cells using a PAM fluorometer (Walz, Germany) plotted against time. Cell abundance was also monitored daily for *C. brevis*, *C. calcitrans*, and *Phaeocystis* sp., by flow cytometry (Accuri C6, BD Biosciences, results not presented). Cultures of *P. globosa*, *P. antarctica* and *C. dichaeta* were examined in 5 mL settling chambers by microscopy (Zeiss Axiovert 25 inverted microscope, results not presented). The PAM fluorometer was used for daily determination of variable vs. maximum fluorescence of photosystem II (F_v/F_m). The experiments were terminated and cells harvested when both cell numbers and fluorescence measurements indicated the exponential growth phase was ending.

3.2 Analysis of nutrients, dissolved iron and iron speciation in the culture media

Concentrations of the dissolved macro nutrients (nitrate + nitrite - termed nitrate for simplicity, phosphate and silicate) were determined on filtered (0.2 µm, 25 mm Acrodisc, Pall Corp) samples using a segmented flow autoanalyzer (Grasshoff et al. 1983; QuAAtro, SEAL Analytical). Samples for nitrate and phosphate were frozen (-20 °C) prior to analysis, while samples for silicate were kept at 4 °C. The detection limit was typically 0.1, 0.01 and 0.1 µmol L^{-1} for nitrate, phosphate and silicate respectively. Total dissolved iron was determined by flow injection analysis with chemiluminescence detection on acidified, filtered (0.2 µm, Sartobran, Sartorius) samples according to the methods described in De Baar et al. (2008). Ligand concentrations and the associated conditional stability constants were determined on filtered samples (0.2 µm) by competitive equilibrium adsorptive cathodic stripping voltammetry (CE-AdCSV) using 2-(2-thiazolylazo)-*p*-cresol (TAC) as the competing ligand (Croot & Johansson 2000). Samples were frozen after collection and defrosted 24 h before analysis. Sample manipulation and data treatment were carried out as described elsewhere (Gerringa et al. 2014).

3.3 Analysis of phytoplankton

Samples for particulate organic carbon (POC), nitrogen (PON), chlorophyll *a* (chl *a*) and heme *b* were collected on glass fiber filters (pore size 0.7 µm, Whatman). Filters for POC and PON were ashed prior to use (400 °C, 8 h). Filters were stored at -20 °C prior to drying (60 °C), and analysis with an elemental analyzer (Carlo Erba NA-1500) standardized using chitin. Chlorophyll *a* was determined by fluorescence against a standard chl *a* solution according to the method of Holm-Hansen et al. (1965).

149 Heme *b* concentrations were determined in phytoplankton after extraction into ammoniacal
150 detergent (Gledhill 2007). In this study we used octyl β-glucopyranoside (OGP) as the detergent,
151 to allow for determination of heme *b* by mass spectrometry (Gledhill 2014). Samples were stored
152 frozen at -80°C prior to analysis. Heme *b* was quantified, after separation from other pigments by
153 high performance liquid chromatography - visible spectrophotometry using a diode array
154 detector (DAD) (Gledhill 2007), and by selectively monitoring the major reactant ion (SRM of
155 m/z = 557) produced by collision induced dissociation of heme *b* (m/z=616) using an ion trap
156 mass spectrometer (ESI-MS, LTQ-Velos, Thermo Scientific) operating in the positive ion mode
157 (Gledhill 2014). Source conditions were optimized, and the instrument tuned using standard iron
158 (III) protoporphyrin IX. Masses were calibrated using the automatic instrument calibration
159 procedure and a standard mass calibration solution (Thermo Scientific). Good agreement was
160 observed between the two detection methods ($[\text{heme}]_{DAD} = 1.06 \times [\text{heme}]_{SRM} + 3.6$ pmol L^{-1},
161 r^2=0.98, *n*=30), with the intercept resulting in a potential difference of <0.3% to the heme
162 concentration in *C. calcitrans* cultures. Concentrations derived from SRM are used in the study,
163 except for *C. calcitrans*, when a problem with the mass spectrometer meant that concentrations
164 were calculated using visible spectrophotometry.

165 Heme *b* growth efficiency was calculated for phytoplankton in culture. Heme growth
166 efficiency is defined in analogy to iron use efficiency after Raven (1988), as the moles of carbon
167 fixed per mole of heme *b* per second. In culture, POC represents a good approximation for
168 phytoplankton carbon and HGE was calculated from the growth rate (s^{-1}) and the heme *b*: POC
169 ratio according to the formula

170 $$HGE = \mu \times \left(\frac{heme\ \mathrm{b}}{POC}\right)^{-1} \quad (1)$$

171 Apparent HGE in three areas of the ocean was also calculated by combining previously
172 published heme *b* concentrations (Gledhill et al. 2013, Honey et al. 2013) with primary
173 productivity data obtained on the same cruises (Table 3; Poulton et al. 2010, Hickman et al.
174 2012, Korb et al. 2012) according to the formula

175 $$apparent\ HGE = \frac{PP(mol\ C\ m^{-2}s^{-1})}{[heme\ \mathrm{b}](mol\ m^{-2})} \qquad (2)$$

176 For field data we add the term "apparent" as there are several uncertainties in both the
177 determination of primary productivity and heme *b* due to approximations made in the
178 calculations, methodological constraints and the complexity of community composition (Honey
179 et al. 2013, Juranek & Quay 2013). Integrated heme *b* concentrations were recalculated to match
180 the depths for the published integrated primary productivity data. Thus, for the Celtic Sea, heme
181 *b* concentrations were integrated over the whole water column and compared to the median total
182 water column primary productivity given in Table 2 from Hickman et al. (2012). In the Scotia
183 Sea, our stations SSC4, SSP24 and SSP28 had mixed layer depths and integrated chl *a*
184 characteristic of "MID", "SW-SG" and "NW-SG" respectively and heme *b* was thus integrated
185 to upper mixed layer depths given in Table 2 of Korb et al. (2012). In order to calculate HGE for
186 the Iceland Basin, heme *b* was integrated to the mixed layer depth given in Table 1 of Poulton et
187 al. (2010).

188 Statistical analysis of results was carried out in the software package Sigmaplot® v12.5
189 using analysis of variance, or non-parametric analysis of variance in cases of non-normal data
190 distributions.

191

4. Results

4.1 Growth rates

Growth rates and F_v/F_m for the five species are presented in Figure 1. The Southern Ocean species had growth rates of up to 0.5 day^{-1} and F_v/F_m up to 0.5 in SOs or SOs+Fe, similar to values reported previously for Southern Ocean species growing near ambient iron concentrations (Timmermans et al. 2004, Hoffmann et al. 2008, Strzepek et al. 2011). In contrast, *Chaetoceros calcitrans* repeatedly failed to grow in SOs or SOs+Fe while *P. globosa* was able to grow in SOs+DFB, SOs and SOs+Fe, albeit with very low growth rates (0.13-0.20 day^{-1}) and with significantly reduced F_v/F_m ($p<0.01$). Consequently these two species were grown in enrichedSOs, with added vitamins, EDTA and trace metals, when growth rates of > 0.7 day^{-1} and F_v/F_m > 0.6 were observed, values more typical for iron replete conditions. No attempt was made to grow the Southern Ocean species in enriched SOs.

4.2 Culture media nutrient and iron concentrations

Concentrations of nitrate, phosphate and silicate in the culture media at the beginning of the experiments were 27.4 ± 1.0, 1.7 ± 0.1 and 64.9 ± 0.7 µmol L^{-1} respectively (n =6). None of the species grown in these experiments completely reduced the nitrate, phosphate or silicate inventories in SOs or SOs+DFB to levels below the detection limit (Table 1). Of the Southern Ocean species, *P. antarctica* consumed the most nitrate, with concentrations of nitrate depleted to levels below detection in SOs+Fe (Table 1). The amount of nitrate converted to PON in each bottle in experiments with no added iron, for experiments with *P. antarctica* was rather variable even though the total nitrogen (i.e. nitrate + PON) calculated for each bottle was close to the concentration of nitrate determined at the start of the experiment (108 ± 14 % for SOs+DFB and

214 97 ± 7 % for SOs). For cultures of *P. globosa* and *C. calcitrans* grown in enrichedSOs, dissolved
215 nitrate was completely removed from the media, and particulate organic nitrogen concentrations
216 were determined to be 95 ± 16 % (*n*=6) and 82 ± 0.04 % (*n*=7) of the starting nitrate
217 concentrations, respectively.

218 Iron concentrations in SOs averaged 0.35 ± 0.17 nmol L^{-1} (n = 5) for the experiments on *C.*
219 *brevis* and *C. dichaeta*, and 0.29 ± 0.01 nmol L^{-1} (n = 3) for experiments on *Phaeocystis* sp. The
220 natural ligand concentrations in SOs were very similar to the iron concentration (0.36 ± 0.03
221 nmol Eq Fe L^{-1} (n=2)) and conditional stability constants ($\log K^{cond}_{FeL_i(Fe^{3+})}$ = 22.4 ± 0.01 mol^{-1}, at
222 20 °C) were typical for open ocean ligands (Gledhill & Buck 2012). Iron concentrations were not
223 measured in enriched SOs treatments. Dissolved iron concentrations and speciation were also
224 determined in SOs treatments at the end of experiments on *P. antarctica* (0.33 ± 0.21, n = 2), *C.*
225 *dichaeta* (0.2 ± 0.03, n = 3) and *P. globosa* (0.36 ± 0.31, n =3). Iron concentrations were thus not
226 significantly reduced during the course of the experiments (t-test, p<0.05). The observed increase
227 in variability was likely indicative of small amounts of iron contamination occurring during the
228 course of the experiment. Similarly, ligand concentrations and stability constants did not change
229 so that the overall average for ligand concentrations at the time that cells were harvested was
230 0.24 ± 0.14 nmol Eq Fe L^{-1} (n = 6) and the $\log K^{cond}_{FeL_i(Fe^{3+})}$ was 22.8 ±0.5, (n=6). A simple ion
231 pairing model (van den Berg 1984) was used to estimate a concentration of approximately 4
232 pmol L^{-1} inorganically complexed iron (Fe´) in SOs.

233 *4.3 Heme* b *concentrations*

234 We present here the heme *b* concentrations (i.e. pmoles heme *b* per liter culture media) at the
235 end of the growth period, in order to relate them to the dissolved iron concentrations in a semi-

quantitative mass balance approach. The lowest particulate heme *b* concentrations were observed in cultures of *C. brevis* in SOs+DFB (Fig. 2). In these *C. brevis* cultures approximately 1.0 ± 0.5 % of the dissolved iron present at the beginning of the experiment was incorporated into heme *b*. Particulate heme *b* concentrations were higher in *C. dichaeta* cultures when compared to the other Southern Ocean species. For *C. dichaeta* cultured in SOs, heme *b* concentrations represented 14 ± 9 % of the total dissolved iron inventory at the start of the experiments. Heme *b* concentrations for *P. antarctica* and *P. globosa* were intermediate in value between *C. brevis* and *C. dichaeta* and no significant differences were observed between SOs, SOs+DFB and SOs+Fe treatments ($p<0.01$) for analysis of variance between treatments within species. Heme *b* concentrations observed in *C. calcitrans* and *P. globosa* cultured in enriched SOs were an order of magnitude higher than heme *b* concentrations observed in unenriched SOs (i.e. cultures grown without added trace metals, EDTA and vitamins), reaching a maximum of 2930 ± 300 pmol L^{-1} for *C. calcitrans* grown with 150 nmol L^{-1} iron (Fig. 2). At total iron concentrations of 15 nmol L^{-1}, *C. calcitrans* incorporated 8 ± 1 % of the total iron inventory into heme *b*.

4.4 Heme b *quotas, heme* b*:chlorophyll* a *ratios and heme growth efficiency*

In this study, heme *b* quotas (µmol heme *b* mol^{-1} C) and heme *b*: chl *a* did not show significant variability between treatments within species (Fig. 3). However, significant differences in heme *b*:C were observed between species when all treatments were pooled ($p<0.01$). Heme *b*:C for *C. brevis* and *P. antarctica* were thus significantly lower than heme *b*:C observed for *P. globosa* and *C. calcitrans*, and also lower than those reported previously for other species (Honey et al. 2013). Heme *b*: C reported for *P. antarctica* compare well (overall average 0.08 ± 0.05 µmol mol^{-1}) with Fe:C ratios of 2.0-2.7 µmol mol^{-1} previously reported for *P. antarctica* grown at similar iron concentrations (Strzepek et al. 2011) given that heme *b* has

been shown to make up between 1 and 40% of the total cellular iron pool in previous studies (Honey et al. 2013). Heme *b*:C and F_v/F_m were weakly correlated (Fig. 4; r=0.55, p<0.01, n=46), as particularly low F_v/F_m was observed for *P. globosa* grown in unenriched SOs treatments. Comparison of heme *b* with particulate organic nitrogen (Table 1) indicated that heme *b*:N ratios increased in treatments where nitrate was completely exhausted.

Heme *b* was also significantly reduced relative to chl *a* for both *P. antarctica* and *C. brevis* compared to *P. globosa* and *C. calcitrans* (Fig. 3B). Heme *b* was observed to be three orders of magnitude lower than chl *a* in these small Southern Ocean species, so that the relative abundances of heme *b* and chl *a* were similar to those observed in particulate material sampled in high latitude, iron deplete waters of the North Atlantic and Scotia Sea (Gledhill et al. 2013). Relative abundances of heme *b* and chl *a* in *C. dichaeta* were intermediate in value, while the relative abundances of heme *b* and chl *a* in *P. globosa* and *C. calcitrans* were similar to those reported previously for *Phaeodactylum tricornutum, Thalassiosira oceanica, T. weissflogii* and *Synechococcus* sp. (Honey et al. 2013). In this study, no significant trends in the relative abundance of heme *b* and chl *a* were observed with changing iron availability.

The impact of changes in heme *b* on growth was examined through calculation of the heme growth efficiency (HGE). Comparison within species indicated that a significantly lower HGE was observed for *C. brevis* and *P. globosa* when grown with low iron availability (Fig. 5). When treatments were pooled (omitting treatments with significantly lower HGE), the small Southern Ocean species *P. antarctica* and *C. brevis* were both observed to have significantly higher HGE than *C. calcitrans* and there was an overall trend of decreasing HGE in the order *P. antarctica* > *C. brevis* > *C. dichaeta* ≈ *P. globosa* ≈ *C. calcitrans*.

We calculated apparent HGE for the Celtic Sea, a coastal, iron replete region (Hickman et al. 2012, Honey et al. 2013), the Iceland Basin (Poulton et al. 2010, Gledhill et al. 2013), a high latitude, seasonally iron limited region (Nielsdottir et al. 2009), and the Scotia Sea (Korb et al. 2012, Nielsdottir et al. 2012), a productive region of the Southern Ocean. Data used in these calculations are presented in Table 2. Integrated heme *b* concentrations were recalculated to match depths for reported integrated primary productivity data (Table 2) and results are presented in Fig. 6. Apparent HGE for the Celtic Sea averaged 2 ± 1 mol C mol heme b^{-1} s^{-1} (n=4), while HGE ranged from 1 to 4.2 mol C mol heme b^{-1} s^{-1} (n=3) in the Scotia Sea and from 1.0 mol C mol heme b^{-1} s^{-1} up to 27 mol C mol heme b^{-1} s^{-1} (n=10) in the high latitude North Atlantic.

5. Discussion

We compared heme *b* concentrations in batch cultures of the Southern Ocean haptophyte *P. antarctica* and the diatoms *C. brevis* and *C. dichaeta* to that in the temperate coastal species *P. globosa* and *C. calcitrans*. We selected *P. globosa* and *C. calcitrans* because they are similar in size to *P. antarctica* and *C. brevis* (cell volumes approximately 100 µm^3 for *Phaeocystis* sp., *C. brevis* and *C. calcitrans* as opposed to approximately 4000 µm^3 for *C. dichaeta*), but they were isolated from coastal environments (North West Europe and Japan, respectively) and thus represented a contrast to the Southern Ocean species with respect to potential iron requirements. It was interesting to note that our coastal species grew very poorly or not at all in unenriched SOs. While the contrasting growth of our Southern Ocean and coastal species in SOs was in accordance with variations in iron requirements reported previously (Timmermans et al. 2005, Hoffmann et al. 2008, Lane et al. 2009, Strzepek et al. 2011), our experiments do not allow us to identify low iron concentrations as the sole cause for the low growth rates of the coastal species,

as multiple trace elements and vitamins were added to the enriched media. Nevertheless, particulate heme *b* concentrations in our experiments increased with iron concentration (Fig. 2) with up to one sixth of dissolved iron converted to heme *b* when iron concentrations were similar to those observed in the ocean. Interestingly, even for *C. calcitrans,* heme *b* concentrations were 8 ± 1 % of the total iron inventory in cultures containing 15 nM dissolved iron, suggesting that a large proportion of the total dissolved iron was utilized by this species at this iron concentration.

Closer examination of the different treatments suggests that there are interspecies differences with respect to the influence of the chemical speciation of iron on heme *b* concentrations. The strong iron chelator DFB reduced growth in *C. brevis* and prevented sustained growth for *C. dichaeta*, but made little difference to the amount of heme *b* produced by *P. antarctica* and *P. globosa* in our experiments. These results agree with previous studies showing that iron in DFB is not universally unavailable to eukaryotic phytoplankton (Strzepek et al. 2011, Shaked & Lis 2012). Furthermore, in our experiments, addition of iron as $FeCl_3$ (SOs+Fe treatments) had only a slight impact on particulate heme *b* concentrations for all the species that grew in SOs+Fe (Fig. 2). This is likely a result of losses of the added iron to the bottle walls or as precipitates, as natural ligands were saturated or very close to saturation in SOs. The contrast between heme *b* concentrations observed with SOs+Fe when compared to experiments with enriched SOs highlights the importance of ligands as iron buffers, keeping iron in solution, and thus potentially available for uptake (Sunda et al. 2005, Gerringa et al. 2012, Thuróczy et al. 2012).

Macro nutrients were underexploited by all species grown in experiments in SOs or SOs+DFB. Enriching SOs with trace metals, a trace metal buffer (EDTA) and vitamins facilitated complete exploitation of macro nutrients in the culture media and coincided with order of magnitude increases in heme *b* concentration. We cannot say with certainty that this increase

in macronutrient utilization resulted from the relief of iron limitation alone as the enriched media involved addition of a suit of trace metals and vitamins in addition to iron. However, an increase in heme *b* could be directly linked to increased exploitation of nitrate in enriched SOs via an increased ability to undertake cytochrome b_{557} dependent assimilatory nitrate reduction. Assimilatory nitrate reduction has previously been shown to be reduced in iron limited phytoplankton (Timmermans et al. 1994). Furthermore heme *b* in assimilatory eukaryotic nitrate reductase is likely to be labile for our extraction protocol (Gledhill et al. 2013, Honey et al. 2013) as the protein is structurally similar to sulfite oxidase (Hille 2013) in which heme *b* is relatively exposed. However, this potential link between heme *b* and nitrate reduction is undermined by results from experiments on *P. antarctica*, which removed all the available nitrate in SOs+Fe, without any observable increase in heme *b* concentrations.

Low iron quotas have previously been observed in Southern Ocean phytoplankton (Hassler & Schoemann 2009, Strzepek et al. 2011). However, the abundance of the intracellular content of more specific iron pools has not previously been widely investigated. Here, we show that small Southern Ocean species also have low heme *b* quotas (Fig. 3). Furthermore, while heme *b* was reduced relative to POC in *P. antarctica* and *C. brevis*, chl *a*:C ratios were not reduced so that the relative abundances of heme *b* and chl *a* were similar to those observed in low iron regions of the Scotia Sea and Iceland Basin (Gledhill et al. 2013). Low heme *b* relative to chl *a* had not been observed in the diatom species examined previously (Honey et al. 2013), but in this study *C. brevis*, a Southern Ocean diatom tolerant to low iron concentrations, also had low heme *b* relative to chlorophyll *a*. This study thus supports previous work that has linked decreases in the abundance of heme *b* relative to chl *a* in the ocean (Honey et al. 2013, Gledhill 2014) to low nutrient availability and the consequent changes in species composition.

Heme *b* is required to fix carbon in eukaryotes as it is a component of the photosystem protein complexes cytochrome b_6f and photosystem II. Previous work has shown a correlation between heme *b* quota and F_v/F_m, the quantum yield of photosystem II (Honey et al. 2013). The weaker correlation observed in this study was highly influenced by the results obtained when *P. globosa* was grown in unenriched SOs. It is possible that *P. globosa* in unenriched SOs was not truly acclimated to the conditions and that this was then reflected in the comparison between F_v/F_m and the heme *b* quota. Nevertheless, the observed trend between F_v/F_m and heme *b* quota does suggest that, in the majority of treatments, there could be a link between a lower quantum yield of PSII and heme *b* quota, and that lower heme *b* may thus impact on growth. In this study, we examined the relationship between growth and heme *b* quotas through calculation of HGE (equation 1). Decreasing HGE suggests that low heme *b* quotas have a direct impact on growth, while higher HGE indicates that the heme *b* quota can be optimized. Reduced HGE was observed at low iron concentrations for *C. brevis* and *P. globosa*, suggesting that decreased heme *b* did result in a growth cost. However, growth rates for *P. antarctica* and *C. brevis* in SOs and SOs+Fe were relatively high (Fig. 1) despite the low intracellular heme *b* concentrations, leading to high HGE (Fig. 5) and suggesting that optimization of heme *b* quota may be a mechasnism by which a species can reduce its iron use whilst maintaining growth at low iron concentrations.

Results for HGE could be influenced by the nature of the extraction protocol used for heme *b* determination. Both protein structure and intracellular localization may impact on heme *b* extraction efficiency. The extraction protocol used in this study has been shown to be biased towards heme *b* molecules that are relatively accessible to attack by solvents (Gledhill et al. 2013, Honey et al. 2013). Examination of crystal structures suggests heme *b* in the photosystem cytochromes b_6 and b_{559} is at least moderately extractable with our protocol (Stroebel et al. 2003,

373 Muh et al. 2008). Furthermore, the heme *b* in cytochrome b_{559} has been shown to be labile in
374 detergent solution at high pH (Weber et al. 2011). Although we cannot state with confidence
375 which hemoprotein pool is impacted by reductions in heme *b*, our observed variations in HGE
376 indicate that reduced heme *b* does not necessarily result in reduced growth and that individual
377 phytoplankton species are likely to optimize iron use by manipulating the intracellular
378 hemoprotein pool.

379 It was notable that in our study *P. antarctica* showed a remarkable ability to both fix carbon
380 and utilize nitrate, despite low intracellular heme *b* concentrations. Our results suggest that
381 species such as *P. antarctica* can produce approximately ten times more particulate carbon than,
382 for example, *P. globosa*, given the same iron and nitrogen resource. Heme *b* makes up an
383 important fraction of the total cellular iron pool. Our work is consistent with previous studies
384 (Strzepek et al. 2011) that have also shown an increase in iron use efficiency in small Southern
385 Ocean species such a *P. antarctica*, even though our experiments did not incorporate such a long
386 adaptation time as Strzepek et al. (2011), and our species may not have been fully acclimated to
387 the low iron treatments. Our work thus suggests that a low heme *b* quota and the ability to
388 exploit a wide variety of iron sources likely contribute to the mechanisms by which *P. antarctica*
389 can efficiently exploit iron inputs (Marsay et al. 2014) in areas such as the Ross Sea, where this
390 species can form large blooms, resulting in the drawdown of CO_2 (Tagliabue & Arrigo 2005).

391 In field samples, heme *b* in non photosynthesizing plankton could potentially act to decrease
392 apparent HGE, and differences in methodologies used to determine primary productivity could
393 also bias our results (Halsey et al. 2010). However, despite these potential offsets, our calculated
394 apparent HGE obtained from heme *b* concentrations and primary productivity determined for
395 coastal (Celtic Sea) and open ocean (High Latitude North Atlantic –HLNA- and Scotia Sea)

396 regions were within the range calculated in our phytoplankton cultures. In the Scotia Sea, HGE
397 was not as high as that observed for *P. antarctica* as the Scotia Sea tends to be dominated by
398 diatoms or dinoflagellates (Korb et al. 2010, Korb et al. 2012). The highest HGE was thus
399 observed in the HLNA at stations characterized by iron concentrations <0.05 nmol L^{-1}, i.e.
400 stations IB285 and IB260 (Gledhill et al. 2013). Thus the lower levels of heme *b* that have been
401 observed in low iron open ocean environments (using this extraction technique) do not
402 necessarily imply low growth or productivity. In fact, increased HGE is necessary in areas with
403 low heme *b* relative to chl *a*, in order to comply with observed correlations between productivity
404 and chlorophyll *a* (e.g. Poulton et al. 2010).

405 In this study we have shown that small, Southern Ocean phytoplankton had low heme *b*
406 quotas. Species with low heme *b* quotas did not necessarily exhibit low growth rates, suggesting
407 that heme *b* quotas were optimized, possibly in order to reduce overall iron requirements. We
408 furthermore compared previously published field data with primary productivity and also found
409 that low heme *b* relative to chlorophyll *a* was not necessarily associated with decreased
410 productivity. Our results suggest considerable variability with respect to heme *b* quotas amongst
411 marine phytoplankton in culture, and that this variability may also be observed in the field. Heme
412 *b* quotas could change as a result of optimization of biological iron pools and also be influenced
413 by methodological constraints imposed by the extraction protocol. Irrespective of the cause, the
414 finding that a particular iron pool is reduced in phytoplankton growing at low iron
415 concentrations, both in the laboratory and in the field, and that the reduction in this important
416 iron pool does not impact proportionately on carbon accumulation, sheds further light on how
417 marine phytoplankton can adapt to low iron, open ocean environments.

418 6. Acknowledgements

419 The authors would like to thank the anonymous reviewers for their constructive comments on the
420 manuscript. MG was supported by a Natural Environment Research Council Advanced Fellowship
421 (NE/E013546/1). The authors would like to thank A. Noordeloos (NIOZ) for her help with PAM
422 fluorescence and flow cytometry, S. Akbari (UoS) for his assistance with POC/N analysis and M.
423 Esposito (UoS) for his assistance with the nutrient analysis.

424

7. References

Croot PL, Johansson M (2000) Determination of iron speciation by cathodic stripping voltammetry in seawater using the competing ligand 2-(2-Thiazolylazo)-p-cresol (TAC). Electoanalysis 12:565-576

De Baar HJW, De Jong JTM (2001) Distribution, sources and sinks of iron in seawater. In: Turner DR, Hunter KA (eds) The biogeochemistry of iron in seawater. Wiley, Chichester

De Baar HJW, Timmermans KR, Laan P, De Porto HH, Ober S, Blom JJ, Bakker MC, Schilling J, Sarthou G, Smit MG, Klunder M (2008) Titan: A new facility for ultraclean sampling of trace elements and isotopes in the deep oceans in the international Geotraces program. Mar Chem 111:4-21

Erdner DL, Price NM, Doucette GJ, Peleato ML, Anderson DM (1999) Characterization of ferredoxin and flavodoxin as markers of iron limitation in marine phytoplankton. Marine Ecology-Progress Series 184:43-53

Espinas NA, Kobayashi K, Takahashi S, Mochizuki N, Masuda T (2012) Evaluation of unbound free heme in plant cells by differential acetone extraction. Plant Cell Physiol 53:1344-1354

Gerringa LJA, Alderkamp A-C, Laan P, Thuróczy C-E, De Baar HJW, Mills MM, van Dijken GL, van Haren H, Arrigo KR (2012) Iron from melting glaciers fuels the phytoplankton blooms in Amundsen Sea (Southern Ocean): Iron biogeochemistry. Deep Sea Research Part II: Topical Studies in Oceanography 71–76:16-31

Gerringa LJA, Rijkenberg MJA, Thuróczy C-E, Maas LRM (2014) A critical look at the calculation of the binding characteristics and concentration of iron complexing ligands in seawater with suggested improvements. Environmental Chemistry 11:114-136

Gledhill M (2007) The determination of heme *b* in marine phyto- and bacterioplankton. Mar Chem 103:393-403

Gledhill M (2014) The detection of iron protoporphyrin (heme b) in phytoplankton and marine particulate material by electrospray ionisation mass spectrometry – comparison with diode array detection. Anal Chim Acta 841:33-43

Gledhill M, Achterberg EP, Honey DJ, Nielsdottir MC, Rijkenberg MJA (2013) Distributions of particulate heme *b* in the Atlantic Ocean and Southern Ocean - implications for electron transport in phytoplankton. Global Biogeochemical Cycles 27:1-11

Gledhill M, Buck KN (2012) The organic complexation of iron in the marine environment: A review. Frontiers in Microbiology 3:69

Grasshoff K, Ehrhardt M, Kremling K (1983) Methods of Seawater Analysis. Verlag Chemie, Weinheim

Halsey K, Milligan A, Behrenfeld M (2010) Physiological optimization underlies growth rate-independent chlorophyll-specific gross and net primary production. Photosynthesis Research 103:125-137

Hassler CS, Schoemann V (2009) Bioavailability of organically bound Fe to model phytoplankton of the Southern Ocean. Biogeosciences 6:2281-2296

Hickman AE, Moore CM, Sharples J, Lucas MI, Tilstone GH, Krivtsov V, Holligan PM (2012) Primary production and nitrate uptake within the seasonal thermocline of a stratified shelf sea. Mar Ecol Prog Ser 463:39-57

Hille R (2013) The molybdenum oxotransferases and related enzymes. Dalton Transactions 42:3029-3042

Hoffmann LJ, Peeken I, Lochte K (2008) Iron, silicate, and light co-limitation of three Southern Ocean diatom species. Polar Biology 31:1067-1080

Hogle SL, Barbeau KA, Gledhill M (2014) Heme in the marine environment: from cells to the iron cycle. Metallomics 6:1107-1120

Holm-Hansen O, Lorenzen CJ, Holmes RW, Strickland JDH (1965) Fluorometric Determination of Chlorophyll. Journal du Conseil 30:3-15

Honey DJ, Gledhill M, Bibby TS, Legiret FE, Pratt NJ, Hickman AE, Lawson T, Achterberg EP (2013) Heme b in marine phytoplankton and particulate material from the North Atlantic Ocean. Mar Ecol Prog Ser 483:1-17

Hopkinson BM, Roe KL, Barbeau KA (2008) Heme uptake by *Microscilla marina* and evidence for heme uptake systems in the genomes of diverse marine bacteria. Appl Env Microbiol 74:6263-6270

Juranek LW, Quay PD (2013) Using triple isotopes of dissolved oxygen to evaluate global marine productivity. Annual Review of Marine Science 5:503-524

Kawachi M, Noel M-H (2005) Sterilization and sterile techniques. In: Anderson RA (ed) Algal culturing techniques. Elsevier, China

Korb RE, Whitehouse MJ, Gordon M, Ward P, Poulton AJ (2010) Summer microplankton community structure across the Scotia Sea: implications for biological carbon export. Biogeosciences 7:343-356

Korb RE, Whitehouse MJ, Ward P, Gordon M, Venables HJ, Poulton AJ (2012) Regional and seasonal differences in microplankton biomass, productivity, and structure across the Scotia Sea: Implications for the export of biogenic carbon. Deep Sea Research II 59-60:67-77

Lane ES, Semeniuk DM, Strzepek RF, Cullen JT, Maldonado MT (2009) Effects of iron limitation on intracellular cadmium of cultured phytoplankton: Implications for surface dissolved cadmium to phosphate ratios. Mar Chem 115:155-162

Marsay CM, Sedwick PN, Dinniman MS, Barrett PM, Mack SL, McGillicuddy DJ (2014) Estimating the benthic efflux of dissolved iron on the Ross Sea continental shelf. Geophysical Research Letters 41:2014GL061684

Muh F, Renger T, Zouni A (2008) Crystal structure of cyanobacterial photosystem II at 3.0 angstrom resolution: A closer look at the antenna system and the small membrane-intrinsic subunits. Plant Physiology and Biochemistry 46:238-264

Nielsdottir M, Bibby TS, Moore CM, Hinz DJ, Sanders R, Whitehouse MJ, Korb RE, Achterberg EP (2012) Seasonal dynamics of iron availability in the Scotia Sea. Mar Chem 130-131:62-72

Nielsdottir MC, Moore CM, Sanders R, Hinz DJ, Achterberg EP (2009) Iron limitation of the postbloom phytoplankton communities in the Iceland Basin. Global Biogeochemical Cycles 23:GB3001

Peers G, Price NM (2006) Copper-containing plastocyanin used for electron transport by an oceanic diatom. Nature 441:341-344

Poulton AJ, Charalampopoulou A, Young JR, Tarran GA, Lucas MI, Quartly GD (2010) Coccolithophore dynamics in non-bloom conditions during late summer in the central Iceland Basin (July-August 2007). Limnol Oceanogr 55:1601-1613

Qi ZH, O'Brian MR (2002) Interaction between the bacterial iron response regulator and ferrochelatase mediates genetic control of heme biosynthesis. Mol Cell 9:155-162

Raven JA (1988) The iron and molybdenum use efficiencies of plant-growth with different energy, carbon and nitrogen-sources. New Phytologist 109:279-287

Raven JA (1990) Predictions of Mn and Fe use efficiencies of phototrophic growth as a function of light availability for growth and of C assimilation pathway. New Phytologist 116:1-18

Richaud C, Zabulon G (1997) The heme oxygenase gene (pbsA) in the red alga Rhodella violacea is discontinuous and transcriptionally activated during iron limitation. Proc Natl Acad Sci USA 94:11736-11741

Roe KL, Hogle SL, Barbeau KA (2013) Utilization of heme as an iron source by marine alphaproteobacteria in the *Roseobacter* clade. Appl Env Microbiol 79:5753-5762

Saito MA, Bertrand EM, Dutkiewicz S, Bulygin VV, Moran DM, Monteiro FM, Follows MJ, Valois FW, Waterbury JB (2011) Iron conservation by reduction of metalloenxyme inventories in the marine diazotroph *Crocosphaera watsonii*. Proc Natl Acad Sci USA 108:2184-2189

Shaked Y, Lis H (2012) Disassembling iron availability to phytoplankton. Frontiers in Microbiology 3

Shekhawat GS, Verma K (2010) Haem oxygenase (HO): an overlooked enzyme of plant metabolism and defence. Journal of Experimental Botany 61:2255-2270

Smith LJ, Kahraman A, Thornton JM (2010) Heme proteins—Diversity in structural characteristics, function, and folding. Proteins: Structure, Function, and Bioinformatics 78:2349-2368

Stroebel D, Choquet Y, Popot JL, Picot D (2003) An atypical haem in the cytochrome b(6)*f* complex. Nature 426:413-418

Strzepek RF, Harrison PJ (2004) Photosynthetic architecture differs in coastal and oceanic diatoms. Nature 431:689-692

Strzepek RF, Maldonado MT, Hunter KA, Frew RD, Boyd PW (2011) Adaptive strategies by Southern Ocean phytoplankton to lesson iron limitation: Uptake of organically complexed iron and reduced iron requirements. Limnol Oceanogr 56:1983-2002

Sunda WG, Huntsman SA (1995) Iron uptake and growth limitation in oceanic and coastal phytoplankton. Mar Chem 50:189-206

Sunda WG, Price NM, Morel FMM (2005) Trace metal ion buffers and their use in culture studies. In: Anderson RA (ed) Algal Culturing Techniques. Elsevier

Sunda WG, Swift DG, Huntsman SA (1991) Low iron requirement for growth in oceanic phytoplankton. Nature 351:55-57

Tagliabue A, Arrigo KR (2005) Iron in the Ross Sea: 1. Impact on CO_2 fluxes via variation in phytoplankton functional group and non-Redfield stoichiometry. J Geophys Res-Oceans 110

Tanaka R, Tanaka A (2007) Tetrapyrrole biosynthesis in higher plants. Annual Review of Plant Biology 58:321-346

Thuróczy C-E, Alderkamp A-C, Laan P, Gerringa LJA, Mills MM, Van Dijken GL, De Baar HJW, Arrigo KR (2012) Key role of organic complexation of iron in sustaining phytoplankton blooms in the Pine Island and Amundsen Polynyas (Southern Ocean). Deep Sea Research Part II: Topical Studies in Oceanography 71–76:49-60

Timmermans KR, Stolte W, de Baar HJW (1994) Iron-mediated effects on nitrate reductase in marine phytoplankton. Marine Biology 121:389-396

Timmermans KR, van der Wagt B, de Baar HJW (2004) Growth rates, half-saturation constants, and silicate, nitrate, and phosphate depletion in relation to iron availability of four large, open-ocean diatoms from the Southern Ocean. Limnol Oceanogr 49:2141-2151

Timmermans KR, van der Wagt B, Veldhuis MJW, Maatman A, de Baar HJW (2005) Physiological responses of three species of marine pico-phytoplankton to ammonium, phosphate, iron and light limitation. Journal of Sea Research 53:109-120

van den Berg CMG (1984) Organic and inorganic speciation of copper in the Irish Sea. Mar Chem 14:201-212

Weber M, Prodohl A, Dreher C, Becker C, Underhaug J, Svane ASP, Malmendal A, Nielsen NC, Otzen D, Schneider D (2011) SDS-facilitated in *vitro* formation of a transmembrane b-type cytochrome is mediated by changes in local pH. Journal of Molecular Biology 407:594-606

Table 1. Concentrations of nitrate, phosphate, silicate, particulate organic carbon (POC), particulate organic nitrogen (PON), chlorophyll *a* (chl *a*) and particulate heme *b* observed in cultures of Southern Ocean (*Phaeocystis antarctica*, *Chaetoceros brevis* and *Chaetoceros dichaeta*) and temperate coastal (*P. globosa* and *C. calcitrans*) phytoplankton species at the end of the experiments. For *P. antarctica* data for nitrate, phosphate, POC and PON are presented individually (n=1), because of high variability between experimental triplicates. Chlorophyll *a* and heme *b* concentrations and all data for other species are given as the mean ± SD for experimental triplicates. <d.l.: less than the detection limit; n.d.: not determined.

	Nitrate (µmol L^{-1})	Phosphate (µmol L^{-1})	Silicate (µmol L^{-1})	POC (µmol L^{-1})	PON (µmol L^{-1})	Chl *a* (nmol L^{-1})	Heme *b* (pmol L^{-1})
				Phaeocystis antarctica			
	15.3	0.91	n.d.	69	10		
SOs	<d.l.	0.17	n.d.	190	25	12±5	8.2±0.5
	5.9	0.40	n.d.	119	22		
	10.9	0.46	n.d.	92	15		
SOs+DFB	1.4	0.05	n.d.	140	32	12±5	10±3
	15.0	0.92	n.d.	70	13		
	0.4	<d.l.	n.d.	284	22		
SOs+Fe	<d.l.	<d.l.	n.d.	114	19	16±5	11±6
	<d.l.	0.10	n.d.	127	18		
				Chaetoceros brevis			
SOs	21.7±1.9	1.35±0.05	63.7±0.8	35±7	3.7±0.8	6.6±2.7	7.7±3.0
SOs+DFB	25.5±0.2	1.58±0.14	65.5±0.5	6.2±1.1	1.1±0.3	1.1±0.4	2.4±0.5
SOs+Fe	16.5±3.4	1.00±0.11	58.2±4.4	36±4	5.9±1.0	13±2	13±3
				Chaetoceros dichaeta			
SOs	12.3±4.2	0.70±0.27	38.0±8.9	52±13	7.3±1.5	6.9±1.6	49±30
SOs+Fe	15.6±1.9	0.75±0.14	43.4±2.3	48±12	7.3±2.1	11±1	47±6
				Phaeocystis globosa			

SOs	24.6±1.0	1.61±0.05	n.d.	16±4	2.6±0.3	1.8±0.6	24±4
SOs+DFB	24.8±0.5	1.64±0.02	n.d.	14±3	1.6±0.1	1.4±0.2	16±1
SOs+Fe	22.0±2.8	1.44±0.16	n.d.	16±4	2.5±0.6	1.8±0.5	35±8
enrichedSOs (9 nM)	<d.l.	<d.l.	n.d.	457±50	29±4	49±3	528±26
enrichedSOs (45 nM)	<d.l.	<d.l.	n.d.	482±11	22.3±1.9	56±4	800±200
			Chaetoceros calcitrans				
enrichedSOs (15 nM)	<d.l.	<d.l.	51.1±0.4	540[1] (n=1)	20[1] (n=1)	61±7	1170±80
enrichedSOs (45 nM)	<d.l.	<d.l.	50.5±0.1	560±34	19±1	63±3	1430±80
enrichedSOs (150 nM)	<d.l.	<d.l.	50.9±2.9	480±140	21±1	76±9	2000±200

[1]Two samples lost during analysis

Table 2. Integrated primary productivity, heme *b* and heme growth efficiency (HGE) calculated from previously published field data.

Station	Integrated primary productivity (mmol C m^{-2} day^{-1})	Integrated heme *b* (nmol m^{-2})	HGE (mol C (mol heme *b*)$^{-1}$ s^{-1})
	Celtic Sea[1]		
B21	201	174	1.1
B22	369	217	1.6
OB1	251	276	0.9
U2	273	103	2.6
	Scotia Sea[2]		
SSC4	17	270	0.6
SSP28	29	114	2.6
SSP3	233	579	4.2
	Iceland Basin[3]		
IB204	17	70	2.8
IB209	11	115	1.1
IB212	23	81	3.2
IB222	10	31	3.7
IB226	41	44	11
IB243	49	76	7.4
IB260	41	19	25
IB274	28	27	12
IB285	65	28	27
IB286	41	59	7.9

1. Median integrated primary productivity data for the whole water column were obtained from Hickman et al. (2012). Integrated heme *b* was calculated from Honey et al. (2013).

2. Primary productivity data was obtained from Korb et al. (2012). We used values for "MID", "SW-SG" and "NW-SG" as these regions had integrated chl *a* values that closely corresponded with values we calculated for integrated chl *a* at stations SSC4, SSP28 and SSP3 respectively. We adjusted our values for integrated heme *b* using the upper mixed layer depth given in Korb et al. (2012).
3. Primary productivity data was obtained from Poulton et al. (2010). Integrated heme *b* from data in Gledhill et al. (2013) was recalculated for depths given in Poulton et al. (2010).

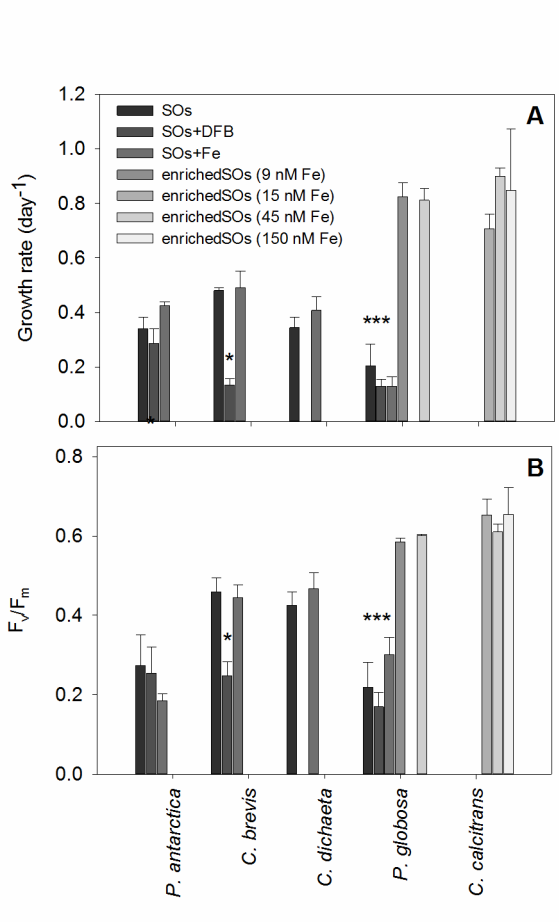

Figure 1. (A) Growth rates (day^{-1}) and (B) F_v/F_m for the Southern Ocean and coastal phytoplankton grown in Southern Ocean seawater (SOs) with added desferrioxamine (DFB), Fe, and trace metals plus ethylenediaminetetraacetic acid (EDTA) (enriched SOs). Southern Ocean species (*Phaeocystis antarctica*, *Chaetoceros calcitrans* and *C. dicheata*) were not grown in enrichedSOs. Growth in SOs+DFB could not be maintained for *Chaetoceros dichaeta*. Values are means ± SD. Significant differences (One way ANOVA on Ranks, $p<0.01$) between treatments within species are denoted by *.

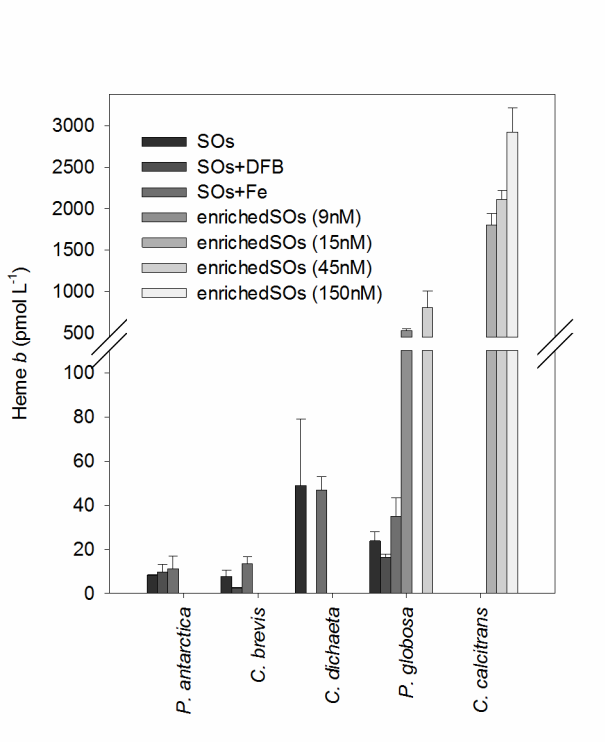

Fig. 2. Heme *b* concentrations (pmol L^{-1}) observed at the end of the exponential phase in Southern Ocean and coastal phytoplankton grown in Southern Ocean seawater treatments. Values are means ± SD.

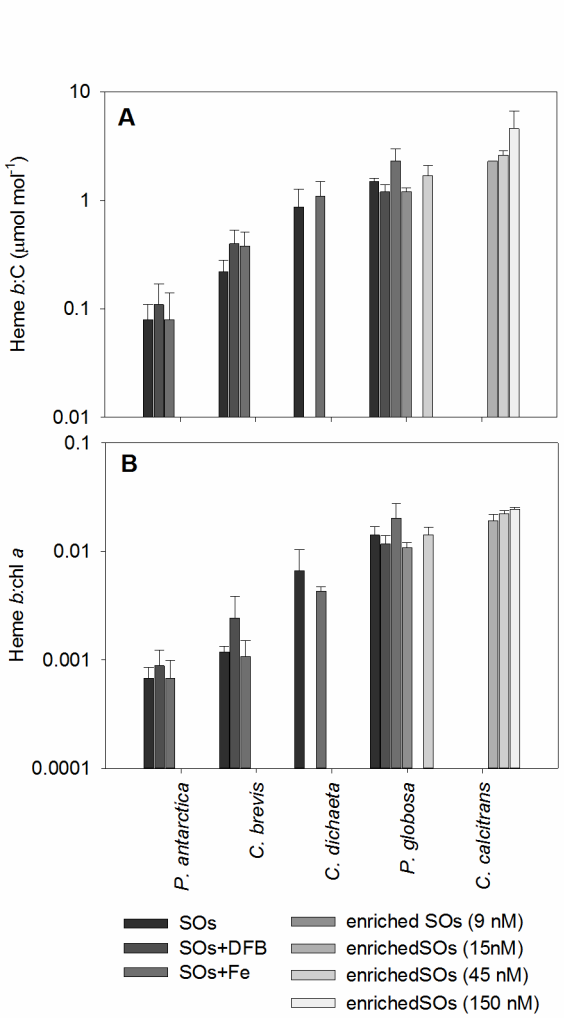

Figure 3. Intracellular heme *b* concentrations expressed relative to (A) carbon (µmol mol^{-1}) in Southern Ocean and coastal phytoplankton species and (B) chlorophyll *a* (expressed as the molar ratio) in Southern Ocean and coastal phytoplankton species. Values are means ± SD. Note log scale on y axis.

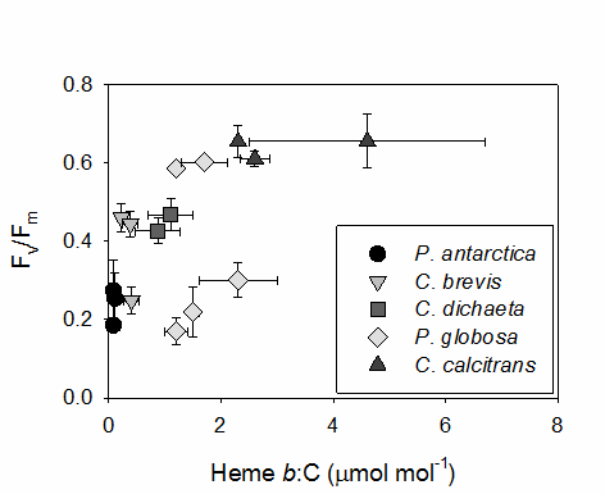

Figure 4. Relationship between heme *b*:C (μmol mol^{-1}) and F_v/F_m in Southern Ocean and coastal phytoplankton species in this study.

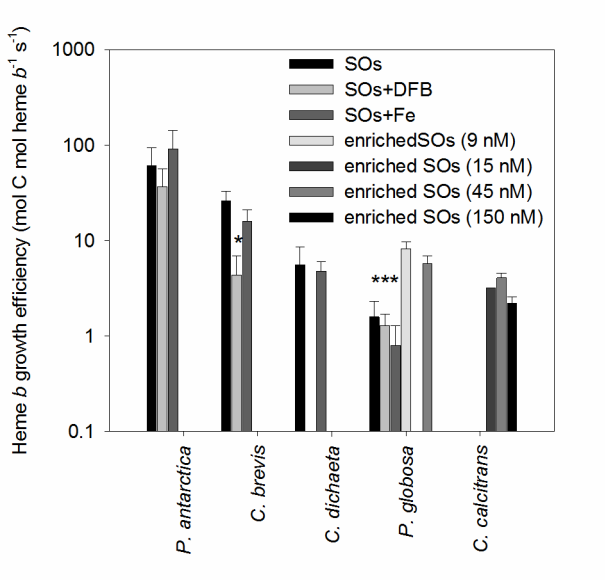

Figure 5. Heme growth efficiency (HGE, mol C mol heme b^{-1} s^{-1}), determined for Southern Ocean and coastal species in our experiments. Values are means ± SD. Significant differences between treatments within species are denoted by * (One way ANOVA on Ranks, $p<0.01$). Note log scale on y axis.

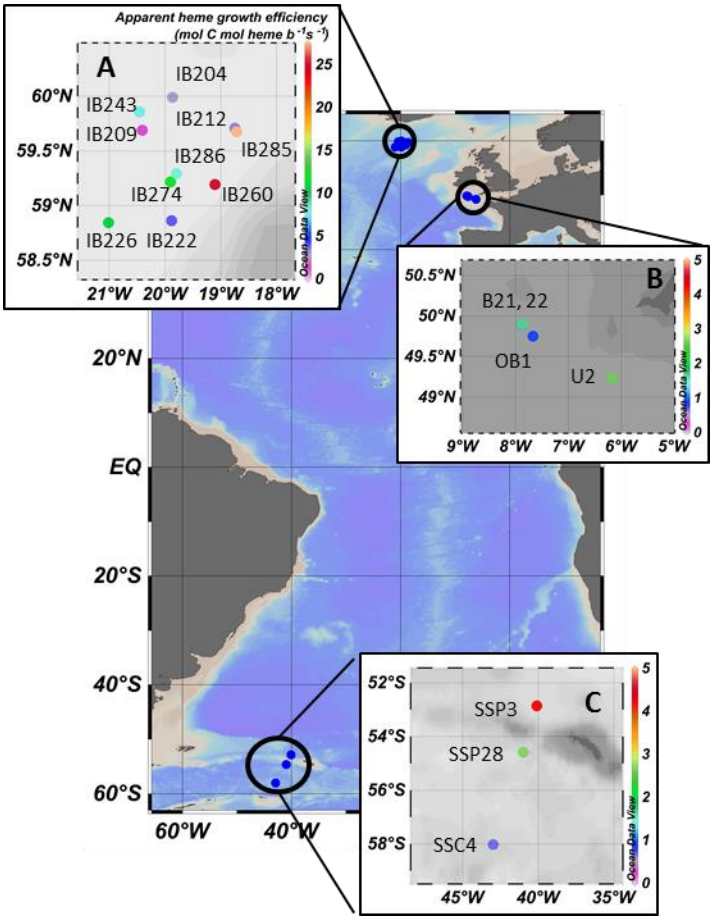

Figure 6. Heme growth efficiency (HGE, mol C mol heme b^{-1} s^{-1}) in (A) the Iceland Basin, (B) the Celtic Sea and (C) the Scotia Sea. HGE was determined for integrated mixed layer depths (Scotia Sea, Iceland Basin) or whole water column depths (Celtic Sea) from previously published productivity data (Poulton et al. 2010, Hickman et al. 2012, Korb et al. 2012) and heme *b* concentrations (Gledhill et al. 2013, Honey et al. 2013). Note scale change for Iceland Basin. Color bar denotes HGE for all inset figures. Background colors represent bathymetry (light grey: 250-2000 m; dark grey: < 250 m)